Progress In Electromagnetics Research Letters, Vol. 44, 35–41, 2014

A Novel Dual-Band Metamaterial Absorber and Its Application for Microstrip Antenna

Hao Zhang*, Xiang-Yu Cao, Jun Gao, Huan-Huan Yang, and Qun Yang

Abstract—In this letter, a novel dual-band metamaterial absorber is presented and analyzed. The absorber is composed of four patches on the top of a thin grounded dielectric substrate which can absorb incident wave at two different frequency bands effectively. Then the absorber is loaded on the dual-band microstrip antenna, whose working frequency bands are overlapped with that of the absorber, to reduce the in-band RCS (Radar Cross Section) of antenna. The prototype is simulated, manufactured and measured. Simulated results show that the absorption of the absorber is as high as 98.6% at 4.29 GHz and 99.8% at 6.49 GHz. As to the dual-band antenna loaded with the proposed absorber, its radiation performance is unchanged while the RCS has declined by 8.59 dB at 4.29 GHz and 9.9 dB at 6.49 GHz respectively. There is a good agreement between simulated and measured results, which verifies that this absorber can be used for in-band RCS reduction of dual-band antenna so as to improve its in-band stealth performance.

1. INTRODUCTION

Recently dual-band antennas have wide applications in many fields such as GPS [1], WLAN [2] and satellite communication [3], while the considerable scattering from dual-band antennas has been the bottleneck in the improvement of the stealth capability of the whole system [4, 5]. The utilization of electromagnetic wave absorber is one of the efficient methods to reduce the Radar Cross Section (RCS) of antennas. Conventional absorbers [6–9] are usually not used to obtain low in-band RCS antennas because of their inherent substantial thickness, heavy weight, lossy surface as well as unstable absorbing performance. The necessity is urged to design a new kind of absorber that can satisfy the demand of in-band RCS reduction of dual-band antennas.

In 2008, Landy [10] proposed a metal-dielectric composite perfect metamaterial absorber (PMA) which is composed of two metallic layers and a dielectric substrate. The design mechanism of PMA is to adjust the effective $\varepsilon(\omega)$ and $\mu(\omega)$ independently by varying the dimensions of electric resonant component and magnetic resonant component in the unit cell so as to match the effective impedance of PMA to the free space and achieve high absorption in the meantime. Compared with the conventional absorbers, this absorber has lots of advantages such as simple manufacture, ultra-thin structure, without lumped resistance and wide applications not only at microwave frequencies but also at THz, infrared and optical bands. Furthermore, several efforts have been made to improve its electromagnetic characteristics, such as polarization-insensitive [11, 12], wide incident angle [13] and dual-band/multi-band absorption [14–16]. The unique advantages of this kind of absorbers bring them to promising alternatives to reduce the RCS of antenna, which has attracted many attentions [17].

In this letter, a novel dual-band metamaterial absorber that can operate at two different frequencies is presented by introducing four different patches in one unit cell. This structure has advantages of high absorption, wide incident angles and polarization-insensitive. Then this absorber is loaded on a dual-band microstrip antenna to reduce its in-band RCS. The prototype is simulated, manufactured and measured. Both simulated and measured results show that the radiation performance keeps well and its in-band RCS declines a lot.

Received 7 September 2013, Accepted 24 November 2013, Scheduled 26 November 2013

* Corresponding author: Hao Zhang (mike303200716008@163.com).

The authors are with the Information and Navigation College, Air Force Engineering University, Xi'an, Shaanxi 710077, China.

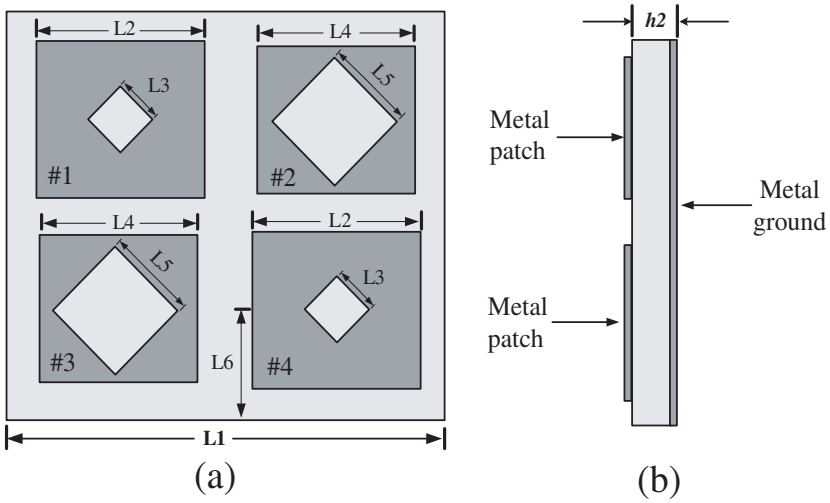

Figure 1. Unit cell geometry. (a) Top view, (b) side view.

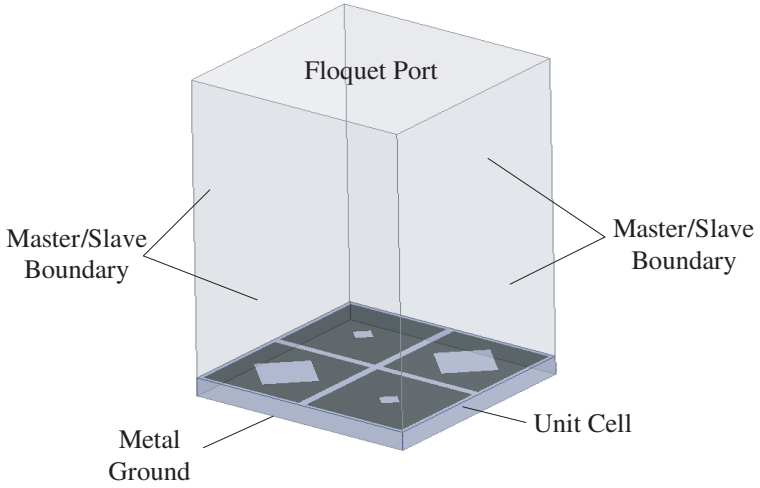

Figure 2. Simulation model.

2. DUAL-BAND ABSORBER DESIGN

Figure 1 shows the unit cell geometry of the proposed absorber. The top layer consists of four square metal patches, and each patch has an oblique square hole in the center. For convenience, these patches are named as #1, #2, #3 and #4 respectively. #1 and #4 have the same size, meanwhile #2 and #3 have the same size. The bottom layer is a solid metal. The dielectric substrate is the FR4 material with $\varepsilon_r = 4.4$ and $\tan\delta = 0.02$. All metals in the absorber are made of copper with the conductivity of $\sigma = 5.8 \times 10^7$ s/m. The absorption is defined as $A = 1 - |S_{11}|^2 - |S_{21}|^2$. Because the proposed absorber is backed by a metallic sheet, i.e., $S_{21} = 0$, the absorption A can be simplified as $A = 1 - |S_{11}|^2$. The model is simulated by using finite-element analysis based on Ansoft HFSS (High Frequency Structure Simulator) as shown in Fig. 2. The Master/Slave boundary conditions and Floquet Port are utilized to simulate the infinite periodic cells. According to optimization of absorption by adjusting geometry, the parameters are given as follows: $L1 = 21.8\,\text{mm}$, $L2 = 10.66\,\text{mm}$, $L3 = 1.65\,\text{mm}$, $L4 = 10.6\,\text{mm}$, $L5 = 7.2\,\text{mm}$, $L6 = 5.45\,\text{mm}$, $h2 = 0.5\,\text{mm}$.

The cases of various incident angles for TE polarization and TM polarization wave have been analyzed as shown in Fig. 3. It can be seen that the absorption peak decreases slightly with the incident angle increasing. But within 40° the peaks keep above 95%.

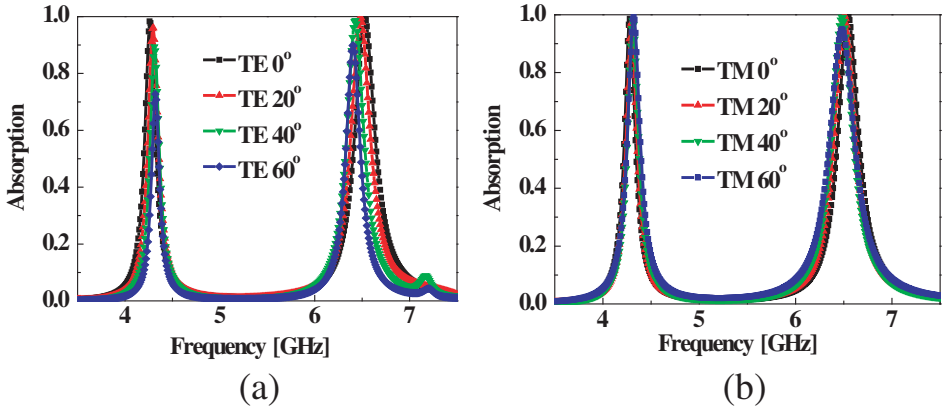

Figure 3. Simulated results of absorption as a function of frequency for different incident angles. (a) TE polarization, (b) TM polarization.

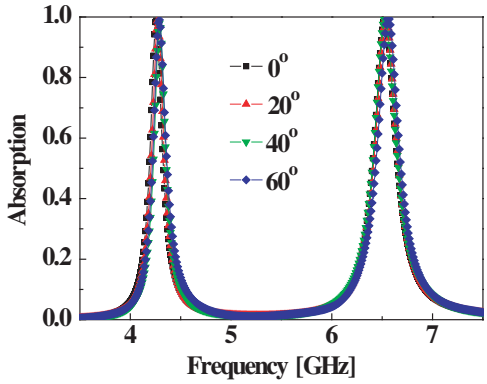

Figure 4. Simulated results of absorption as a function of frequency for different polarization angles.

Figure 4 shows the absorption of different polarization angles. It is observed that different polarization angles have little influence on the absorption, indicating that this absorber is polarization-insensitive.

3. DESIGN OF LOW-RCS MICROSTRIP ANTENNA

The dual-band microstrip antenna is portrayed in Fig. 5. This antenna can work at 4.29 GHz and 6.49 GHz due to two slots on the radiation patch. The dielectric substrate is FR-4 with $\varepsilon_r = 2.65$ and $\tan\delta = 0.02$. The parameters of the antenna are as follows: $a = 109\,\text{mm}$, $b = 20\,\text{mm}$, $c = 0.5\,\text{mm}$, $d = 0.5\,\text{mm}$, $e = 0.5\,\text{mm}$, $l = 2.7\,\text{mm}$, $h = 1\,\text{mm}$.

Based on the property of ultra-thinness, the absorber is loaded on the top of the substrate with a proper distance from the radiation patch as shown in Fig. 6. In this way, the radiation performance can be kept well and the incident wave can be absorbed effectively.

3.1. Radiation Performance

In order to demonstrate the radiation performance, the reflection coefficient S_{11} and radiation patterns were measured by vector network analyzer Agilent N5230C in microwave anechoic chamber.

Figure 7 shows the measured results of S_{11}. It can be seen that the working frequencies of antenna are 4.29 GHz and 6.49 GHz respectively. It can also be got that S_{11} of the antenna keeps unchanged generally after loaded with absorber.

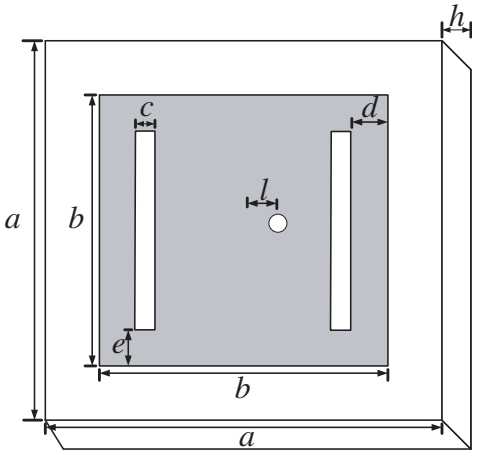

Figure 5. Dual-band microstrip antenna.

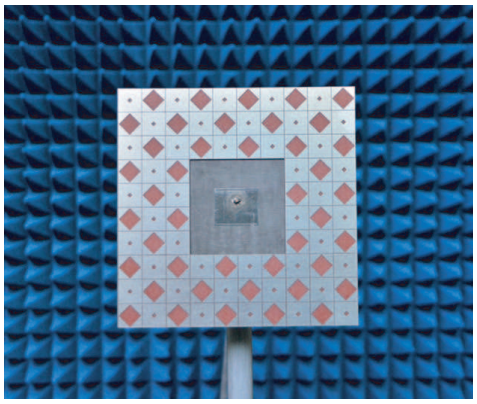

Figure 6. Photograph of designed antenna loaded with absorber.

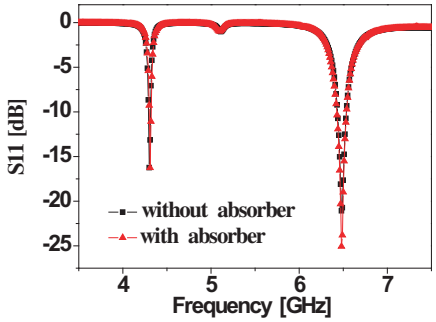

Figure 7. Measured results of S_{11} as a function of frequency.

The radiation patterns of the antennas in both E and H-planes at 4.29 GHz and 6.49 GHz are presented in Fig. 8. It can be seen that the front gain of E- and H-planes keeps well while the backlobe and sidelobe levels fluctuate because the current distribution on the surface of dielectric substrate has been changed by the loaded absorber.

Figure 9 shows the measured results of antenna's gain during two working frequencies. It can be observed that the antenna's gain has declined by 0.47 dB at 4.29 GHz and increased by 0.3 dB at 6.49 GHz, respectively, after loaded with absorber. Meanwhile, in the two working frequency bands, the difference of gain between original and designed antennas is below 1 dB, demonstrating that the designed antenna maintains a good radiation performance.

3.2. Reduction of Antenna's RCS

The simulated monostatic RCS (MRCS) as a function of frequency for normally incident plane wave is shown in Fig. 10.

It can be inferred that the RCS of the antenna has obviously declined within the two operating frequency bands. The RCS is reduced as large as by 8.59 dB of TE polarization and 6.7 dB of TM polarization from 4 GHz to 5 GHz. In $6 \sim 7$ GHz, the RCS is reduced as large as by 9.9 dB of TM polarization and 8.5 dB of TM polarization. It is concluded that the working frequency of absorber is overlapped with that of antenna and the RCS reduction of TE polarization is much better than that of TM polarization.

Figure 11 shows the simulated results of RCS with different incident angles. It can be observed that the RCS has declined efficiently within $-15^\circ \sim +15^\circ$.

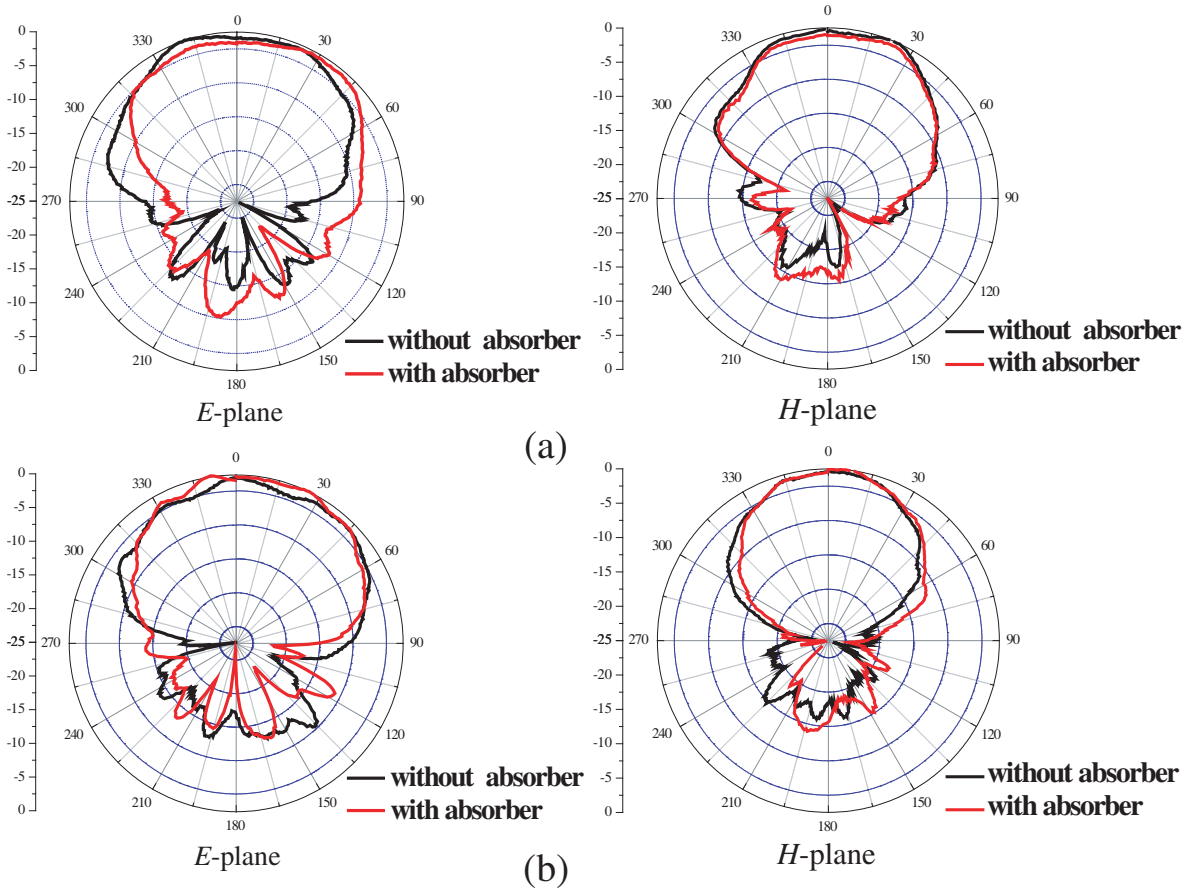

Figure 8. Measured results of radiation patterns at (a) 4.29 GHz, (b) 6.49 GHz.

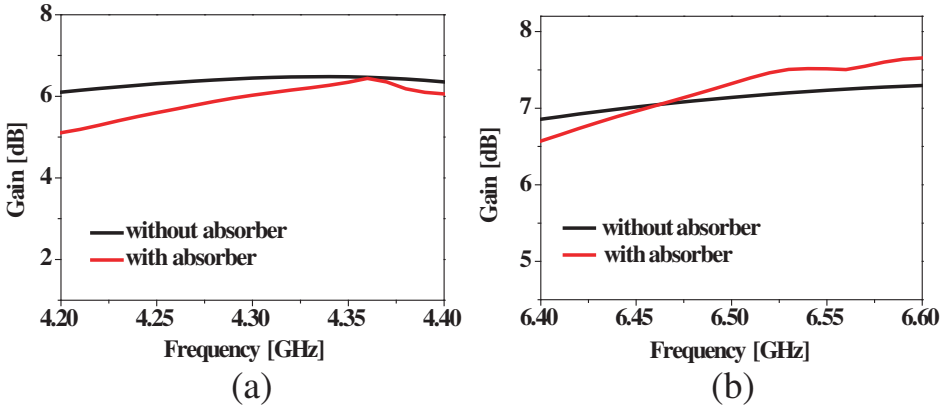

Figure 9. Measured results of gain as a function of frequency. (a) 4.2 GHz–4.4 GHz, (b) 6.4 GHz–6.6 GHz.

Finally, the RCS of two antennas for normal incidence is measured in microwave anechoic chamber. Two horn antenna probes working in $3 \sim 18$ GHz have been chosen as emitter and receiver respectively and all of them are connected to network analyzer Agilent N5230C. The separation between each probe is 2 m to avoid mutual coupling. The far-field distance L can be estimated as $L = 2D^2/\lambda = 0.56$ m, where D is the size of designed antenna ($D = 10.9$ cm) and λ is the wavelength corresponding to the up limit of the frequency band (7 GHz, $\lambda = 4.28$ cm) to make sure that the scattered field is acquired in the far-field region [18].

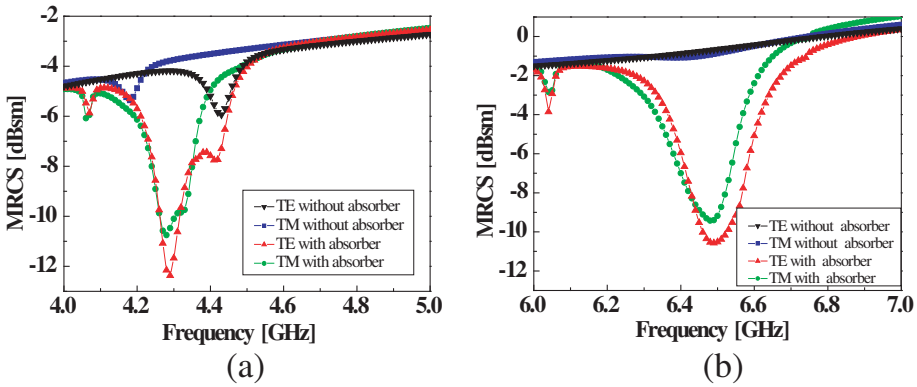

Figure 10. Simulated results of monostatic RCS as a function of frequency. (a) 4 $\sim$ 5 GHz, (b) 6 $\sim$ 7 GHz.

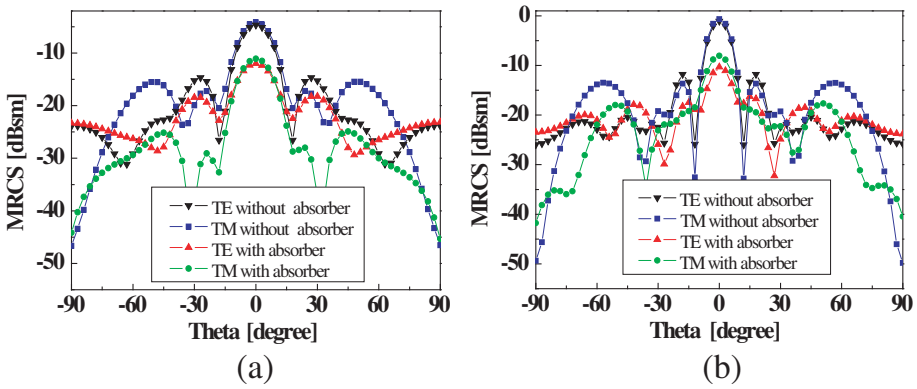

Figure 11. Simulated results of monostatic RCS as a function of incident angles at (a) 4.29 GHz, (b) 6.49 GHz.

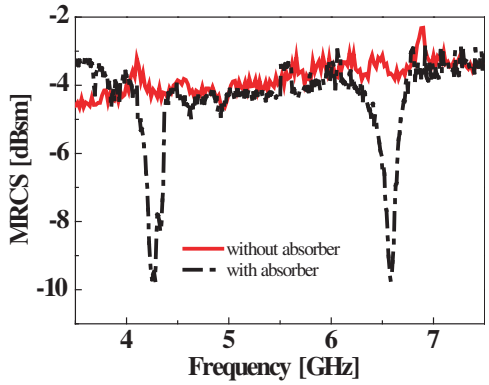

Figure 12. Measured results of monostatic RCS as a function of frequency.

The measured monostatic RCS of the two antennas is shown in Fig. 12. It is seen that the RCS of designed antenna is reduced obviously within its working bands, which verifies the feasibility of the proposed absorber.

4. CONCLUSIONS

A novel dual-band metamaterial absorber is presented in this work. This absorber can achieve high absorption in two different frequencies. Then the absorber is loaded in dual-band microstrip antenna whose working frequency bands are overlapped with that of the absorber to reduce the RCS. The prototype is simulated, manufactured and measured. Both simulated and measured results show that the radiation performance of antenna has not been influenced significantly and the RCS has declined a lot, which makes it an effective way to improve the stealth capability of dual-band antennas.

REFERENCES

1. Chen, M. and C. C. Chen, "A compact dual-band GPS antenna design," *IEEE Antennas Wirel. Propag. Lett.,* Vol. 12, 245–248, 2013.
2. Chow, H. Y., Y. D. Sim, and C. H. Lee, "Compact size dual-band antenna printed on flexible substrate for WLAN operation," *Proceedings of ISAP*, 1047–1050, Nagoya, Japan, 2012.
3. Chiu, C. N. and W. H. Chuang, "A novel dual-band antenna for a satellite and terrestrial communication system," *IEEE Antennas Wirel. Propag. Lett.,* Vol. 8, 624-626, 2009.
4. Knott, E. F., J. F. Shaeffer, and M. T. Tuley, *Radar Cross Section*, 2nd Edition, SciTech Publishing, Inc, Raleigh, NC, 2004.
5. Zheng, J.-H., Y. Liu, and S.-X. Gong, "Aperture coupled microstrip antenna with low RCS," *Progress In Electromagnetics Research Letters,* Vol. 3, 61–68, 2008.
6. Miao, Z. L., C. Huang, X. Ma, and M. B. Pu, "Design of a patch antenna with dual-band radar cross-section reduction," *Microwave and Optical Technology Letters,* Vol. 54, 2516–2520, 2012.
7. Ronald, L. F. and T. M. Michael, "Reflection properties of the Salisbury screen," *IEEE Trans. on Antennas and Propagat.,* Vol. 36, 1443–1454, 1988.
8. Chambers, B. and A. Tennant, "Optimised design of Jaumann radar absorbing materials using a genetic algorithm," *IEE Proc. — Radar, Sonar Navig.*, Vol. 143, 23–30, 1996.
9. Reinert, J., J. Psilopoulos, J. Grubert, and A. F. Jacob, "On the potential of graded-chiral dallenbach absorbers," *Microwave and Optical Technology Letters*, Vol. 30, 254–257, 2001.
10. Landy, N. I., "Perfect metamaterial absorber," *Phys. Rev. Lett.*, Vol. 100, 207402, 2008.
11. Landy, N. I., C. M. Bingham, T. Tyler, N. Jokerst, D. R. Smith, and W. J. Padilla, "Design, theory and measurement of a polarization-insensitive absorber for terahertz imaging," *Phys. Rev.*, Vol. 79, 125104, 2009.
12. Luukkonen, O., F. Costa, A. Monorchio, and S. A. Tretyskov, "A thin electromagnetic absorber for wide incidence angles and both polarizations," *IEEE Trans. Antennas Propag.,* Vol. 57, 3119, 2009.
13. Li, L., Y. Yang, and C. H. Liang, "A wide-angle polarization-insensitive ultra-thin metamaterial absorber with three resonant modes," *J. Apple. Phys.*, Vol. 100, 063702, 2011.
14. Tao, H., C. M. Bingham, A. C. Strikwerda, D. Pilon, et al., "Highly flexible wide angle of incidence terahertz metamaterial absorber: Design, fabrication and characterization," *Phys. Rev.,* Vol. 78, 241103, 2008.
15. Cheng, Y. Z., Y. Wang, Y. Nie, Z. Gong, and X. Xiong, "Design, fabrication and measurement of a broadband polarization-Insensitive metamaterial absorber based on lumped elements," *J. Apple. Phys.,* Vol. 111, 044902, 2012.
16. Ye, Y. Q., Y. Jin, and S. L. He, "Omnidirectional, polarization-insensitive and broadband thin absorber in the terahertz regime," *J. Opt. Soc. Am.*, Vol. 27, 498–504, 2012.
17. Liu, T., X. Y. Cao, J. Gao, Q. R. Zheng, W. Q. Li, and H. H. Yang, "RCS reduction of waveguide slot antenna with metamaterial absorber," *IEEE Trans. Antennas Propag.*, Vol. 61, 1479–1484, 2013.
18. De Cos, M. E. and Y. Alvarez, "Novel SHF-band uniplanar artificial magnetic conductor," *IEEE Antennas Wirel. Propag. Lett.*, Vol. 9, 44–47, 2010.